IPP-Report

IPP Max-Planck-Institut für Plasmaphysik

Kurt Behringer

Escape Factors for Line Emission and Population Calculations

IPP 10/11
April 1998

Escape Factors for Line Emission and Population Calculations

Abstract.

Escape factors for spectral line emission along a given line-of-sight, Θ_L, and for collisional-radiative population calculations of excited levels in atoms and ions, Θ_p, have been calculated on the basis of some simplifying approximations by means of a PC computer program. A wide choice of spectral line profiles, spatial emission profiles and plasma geometry cases is available in the code. Doppler, Lorentz or Holtsmark profiles can be used, as well as convolutions and superposition of different types and widths, in order to account for various line broadening mechanisms and particle groups with different temperatures. The spatial emission profiles of radiation are approximated by a polynomial fit and examples are given for constant emission, as well as a linear or a parabolic decrease from the plasma centre to the edge. The population escape factor can be calculated in the centre of a plasma sphere, in the mid-plane of a disk, or on the axis of a cylinder. The underlying definitions of the escape factor analysis are presented and the approximations in the solution of the equation of radiative transfer are explained. Normalised escape factors for Θ_L and Θ_p for the described cases are shown and the consequences of the different models discussed. The results are applied to a measurement of the neutral hydrogen density from the self-absorption of L_β in ASDEX Upgrade divertor I. For this purpose, a calculation of the L_β line profile is used, which includes Zeeman splitting for the relevant magnetic field and Stark broadening for the plasma electron density. The geometrical form of the emission zone and of the neutral hydrogen cloud are taken from model calculations of the ASDEX divertor plasma. The result for the neutral hydrogen density is in very good agreement with plasma simulations confirming the reliability of such an analysis. In the past, the described program has already been applied to many other studies of opacity including the calculation of ionisation, recombination and radiation coefficients on the basis of the ADAS atomic data base. A special example is presented here, namely, hydrogen net recombination factors for divertor modelling as a function of electron temperature and density, of ionisation degree and of optical thickness of the resonance lines. The essential content of the escape factor program is being added to the ADAS program library.

1. Introduction

The optical thickness of resonance lines plays an important role in many laboratory plasmas, e.g. low-density, low-temperature discharges for plasma technology. However, radiative transfer in hydrogen resonance lines has also become an important issue in present-day divertor plasmas, as e.g. realised in ASDEX Upgrade, due to strong net volume recombination resulting in high neutral densities. This opacity affects the emitted radiance of spectral lines, but also changes the population of excited states and the effective collisional-radiative ionisation and recombination rate coefficients. In order to deal with the consequences of radiative transfer, the escape factor method has been widely used in astrophysics and plasma physics (see e.g. Irons [1] for an overview). In the following report, a relatively simple evaluation and application of escape factors will be discussed for both interpreting optically thick line emission and for dealing with the change in excited state population due to re-absorption of radiation. The basic model described here was implemented in a PC computer code quite some time ago and applied to the study of an air-like plasma jet [2, 3]. The code has been amended and extended since, and a later versions has been used for analysing opacity problems in low-temperature divertor plasmas [4]. Various models for plasma geometry and spectral line profiles have been made available in the course of time. The numerical program had originally been written in BASIC for DOS, and was later translated to Visual Basic for WINDOWS 95, which offers more convenient interactive parameter control by means of predefined objects. It consists of the module "adasescape.bas", a library with plot routines and a few other utilities, as well as some specially-tailored form objects for input and output. The essential content of the program is presently being added to the ADAS atomic physics package [5].

2. Basic Equations and Simplifying Approximations

2.1 Definition of Escape Factors

The spectral radiance $L_\lambda(\lambda)$ in a plasma along a line of sight ℓ is given by the equation of radiative transfer (without scattering):

$$\frac{dL_\lambda}{d\ell} = \varepsilon_\lambda - \alpha' L_\lambda, \tag{1}$$

where ε_λ is the spectral emission coefficient and α' is the effective absorption coefficient, which is obtained by subtracting stimulated emission from absorption. If the population ratio of upper and lower states can be described by a Boltzmann distribution according to the temperature T, α' is given by $\alpha\left[1-exp\left(-\frac{h\nu}{kT}\right)\right]$. For the present application to vuv resonance lines ($h\nu > 10$ eV) and low temperatures, this correction is small and may be even smaller due to underpopulation of the excited states. Therefore, stimulated emission will be neglected in the following discussion, i.e. α' will be replaced by α. The spectral emission coefficient within a spectral line can be derived from the line emission coefficient ε_L and the spectral line profile $P_\lambda(\Delta\lambda)$, which must be calculated on the basis of the relevant line broadening

mechanisms in the plasma:

$$\varepsilon_\lambda(\lambda) = \varepsilon_L P_\lambda(\Delta\lambda), \qquad \varepsilon_\lambda(\lambda) = \frac{n_k A_{kj} h\nu}{4\pi} P_\lambda(\Delta\lambda). \tag{2}$$

In Eq. 2, n_k is the number density in the upper state k and A_{kj} the transition probability to state j. $\Delta\lambda$ is the wavelength distance to the line centre. If the plasma extends over the co-ordinate ℓ from zero to b, the escaping radiance at b is

$$L_\lambda(b) = \int_0^b \varepsilon_\lambda(\ell) \exp\left[-\int_\ell^b \alpha(\ell')\, d\ell'\right] d\ell + L_\lambda(0) \exp\left[-\int_0^b \alpha(\ell)\, d\ell\right]. \tag{3}$$

In the following, the assumption will be made that α is independent of ℓ and equal to $\overline{\alpha}$. In essence this means that the neutral density is constant in the plasma, which is very true for low-density plasmas and probably a good first approximation to the conditions in detached divertor plasmas, which will be dealt with later. Still, it is probably the most restricting condition of the present escape factor discussion. Equation 3 then writes for $L(0) = 0$:

$$L_\lambda(b) = \int_0^b \varepsilon_\lambda(\ell) \exp\left[(\ell - b)\overline{\alpha}\right] d\ell. \tag{4}$$

As a further simplification, we adopt a spatially constant line profile P_λ for both emission and absorption. Again, this limitation should not be too severe for cold divertor plasmas, where P_λ is determined by the thermal motion of the neutral particles on the basis of their Franck-Condon energy or charge exchange temperature, and where the mean-free path of these particles is long compared to the plasma dimensions. In principle, the presented code could be restructured to take into account the spatial variation of the spectral line profiles. The absorption coefficient is then given by the Ladenburg relation

$$\alpha(\Delta\lambda) = \alpha_t P_\lambda(\Delta\lambda), \qquad \alpha(\Delta\lambda) = n_j \frac{g_k}{g_j} \frac{\lambda^4}{c} \frac{A_{kj}}{8\pi} P_\lambda(\Delta\lambda) \tag{5}$$

with the statistical weights g and the Einstein coefficient A_{kj}. α_t is the wavelength-integrated absorption coefficient (nm/cm). The absorption coefficient in the line centre $\alpha(0)$ is of course equal to $\alpha_t P_\lambda(0)$. The escape factor for the integral line emission in the direction of ℓ can now be defined by relating the spectral integral over the self-absorbed line profile to the optically thin line radiance. Later-on, b will be defined as the distance from the plasma edge to the plasma centre, therefore the line-of-sight integral must extend over $2b$:

$$\Theta_L = \frac{\int_0^{2b} \int_{line} \varepsilon_\lambda(\ell, \lambda) \exp\left[(\ell - 2b)\overline{\alpha}(\lambda)\right] d\lambda\, d\ell}{\int_0^{2b} \varepsilon_L(\ell)\, d\ell}$$

viz.
$$\Theta_L = \frac{\int_0^{2b} \varepsilon_L(\ell) \int_{line} P_\lambda(\Delta\lambda) \exp\left[(\ell - 2b)\,\overline{\alpha}_t\, P_\lambda(\Delta\lambda)\right] d\Delta\lambda\, d\ell}{\int_0^{2b} \varepsilon_L(\ell)\, d\ell}. \qquad (6)$$

The line escape factor θ_L in Eq. 6 describes the emitted radiance along a given line-of-sight, as required for spectroscopic measurements. It only depends on the spatial profiles over this one co-ordinate and not on the rest of the plasma geometry. For obtaining the total escaping flux, (another common definition of θ), Eq. 6 must be integrated over solid angle and then requires more information on the plasma shape.

In order to calculate the change in excited state population due to absorption of radiation, absorption is treated as negative emission and the absorption rate is taken into account by subtracting it from the spontaneous emission rate, i.e. by reducing the transition probability A in collisional-radiative model calculations. An effective reduced A-value $A_{eff} = \Theta_p\, A$ is introduced, where Θ_p is determined by the relative difference between the emitted and the absorbed photon numbers (or line radiation powers) E and G:

$$\Theta_p = \frac{E - G}{E} = 1 - \frac{G}{E}. \qquad (7)$$

The number of absorption processes in the plasma per unit volume and time G must be evaluated from the spectral radiance $L_\lambda(\lambda)$ at the relevant plasma location x times the effective absorption coefficient $\alpha'(x, \lambda)$ - again replaced by $\alpha(x, \lambda)$ - , integrated over wavelength and solid angle Ω. For the emitted power, the double integration simply yields 4π times the line emission coefficient $\varepsilon_L(x)$. The spectral radiance usually depends on the individual directions in the plasma, as characterised by the solid angle element $d\Omega$:

$$\Theta_p = 1 - \frac{\int_\Omega \int_{line} \alpha(x,\lambda)\, L_\lambda(x,\lambda,\Omega)\, d\lambda\, d\Omega}{4\pi\, \varepsilon_L(x)} \qquad (8)$$

We restrict this calculation to the plasma centre or the plasma axis and adopt a point or line symmetry for the plasma parameters. If the population is evaluated for position $\ell = b$ in the centre of the plasma and the plasma edge is at $\ell = 0$, where $L_\lambda = 0$, Eq. 4 can be used again:

$$\Theta_p = 1 - \frac{\int_\Omega \int_{line} \alpha(b,\lambda) \int_0^b \varepsilon_\lambda(\ell,\lambda) \exp\left[(\ell - b)\,\overline{\alpha}(\ell,\lambda)\right] d\ell\,(\Omega)\, d\lambda\, d\Omega}{4\pi\, \varepsilon_L(b)} \qquad (9)$$

Since α was set constant, $\alpha(b,\lambda)$ is of course equal to $\overline{\alpha}(\lambda)$. For a given line profile, both θ_L and θ_P only depend on the product of the absorption coefficient in the line centre $\overline{\alpha}(0)$ and the length b, which can be shown as follows: They represent integrals over P_λ times functions of $(\alpha_t P_\lambda\, b)$. The normalised profiles with width w can be written as functions of w and the wavelength distance to the line centre $\Delta\lambda$:

$$P(\Delta\lambda, w) = \frac{1}{w} V\left(\frac{\Delta\lambda}{w}\right). \qquad (10)$$

Introducing $z = \frac{\Delta\lambda}{w}$:

$$\int_{-\infty}^{\infty} P(\Delta\lambda) f\left(\alpha_t P(\Delta\lambda) b\right) d\Delta\lambda = \int_{-\infty}^{\infty} V(z) f\left(\frac{\alpha_t b}{w} V(z)\right) dz, \qquad (11)$$

which means that the integrals only depend on $\frac{\alpha_t b}{w}$, i.e. on $\overline{\alpha}(0)b$. In the program "adasescape", the calculations are being carried out for a specific example, namely, for a wavelength λ = 100 nm, for an absorption oscillator strength of 1, and for a Doppler width according to the input gas temperature and the element mass (w_D = 7.7 pm for hydrogen with mass 1 and 1 eV temperature). This was originally intended for a check of the absolute results after each step, however, the calculations are being normalised to $\overline{\alpha}(0)b$ later in the program and the parameters above just define the range of optical thickness, together with the neutral densities of the density loop. The functions $\Theta_L(\overline{\alpha}(0)b)$ and $\Theta_p(\overline{\alpha}(0)b)$ need not be recalculated each time, but could in principle be tabulated for the various cases required. Applying the escape factors to the modification of transition probabilities in ADAS adf04 data sets, the program uses the standardised results and carries out a quadratic, logarithmic interpolation on the basis of the relevant wavelengths, profiles and A-values in the adf04 files (see description below).

2.2 Spatial Intensity Profiles

The spectral radiance in the relations for both θ_L and θ_P has been worked out by a polynomial fit to the spatial profile of the emission coefficient and by integrating Eq. 4 by parts:

$$L_\lambda(b) = \int_0^b \varepsilon_\lambda(\ell) \exp\left[\overline{\alpha}(\ell - b)\right] d\ell = \frac{\varepsilon_\lambda(b)}{\overline{\alpha}} - \frac{\varepsilon'_\lambda(b)}{\overline{\alpha}^2} + \frac{\varepsilon_\lambda''(b)}{\overline{\alpha}^3} - \ldots$$

$$- \exp(-\overline{\alpha}b)\left(\frac{\varepsilon_\lambda(0)}{\overline{\alpha}} - \frac{\varepsilon'_\lambda(0)}{\overline{\alpha}^2} + \frac{\varepsilon''_\lambda(0)}{\overline{\alpha}^3}\right) - \ldots, \qquad (12)$$

where ε'_λ means the first derivative with respect to ℓ etc..

Three spatial intensity profiles have been investigated: (e1) constant emission over ℓ, (e2) a linear increase from the edge to the plasma centre, and (e3) a parabolic shape with its maximum in the plasma centre. The results of the integration over ℓ are shown in Table 1. In cases (e2) and (e3), $\varepsilon_\lambda(b)$ is the value in the plasma centre, $\varepsilon_\lambda(0) = \varepsilon_\lambda(2b) = 0$. The optically thin line spectral radiances for a line-of-sight from 0 to $2b$ and for the three spatial profiles are $2b\varepsilon_\lambda$, $b\varepsilon_\lambda$ and $\frac{4}{3}b\varepsilon_\lambda$, respectively, and the same factors apply, of course, to the wavelength-integrated radiances. If α approaches zero (almost optically thin), the exponential functions in Table I must possibly be expanded to avoid numerical overflow.

Table 1: Optically thick spectral radiances for (e1) spatially constant emission, (e2) linear increase from the edge to the centre and (e3) parabolic emission profile.

case	integration from 0 to b (centre); $L_\lambda(b)$	integration from 0 to $2b$ (edge); $L_\lambda(2b)$
e1	$\frac{\varepsilon_\lambda}{\overline{\alpha}}\left[1-\exp(\overline{\alpha}b)\right]$	$\frac{\varepsilon_\lambda}{\overline{\alpha}}\left[1-\exp(-\overline{\alpha}2b)\right]$
e2	$\frac{\varepsilon_\lambda(b)}{\overline{\alpha}}\left(1-\frac{1}{\overline{\alpha}b}+\frac{1}{\overline{\alpha}b}\exp(-\overline{\alpha}b)\right)$	$\frac{\varepsilon_\lambda(b)}{\overline{\alpha}}\frac{1}{\overline{\alpha}b}\left[1-2\exp(-\overline{\alpha}b)+\exp(-2\overline{\alpha}b)\right]$
e3	$\frac{\varepsilon_\lambda(b)}{\overline{\alpha}}\left[1-\frac{2}{\overline{\alpha}^2b^2}+\left(\frac{2}{\overline{\alpha}b}+\frac{2}{\overline{\alpha}^2b^2}\right)\exp(-\overline{\alpha}b)\right]$	$\frac{\varepsilon_\lambda(b)}{\overline{\alpha}}\frac{1}{\overline{\alpha}b}\left[2-\frac{2}{\overline{\alpha}b}+\left(2+\frac{2}{\overline{\alpha}b}\right)\exp(-2\overline{\alpha}b)\right]$

Using the above results, the line escape factor for case (e1) is e.g.:

$$\Theta_L = \int_{line}\frac{P_\lambda}{2\,\overline{\alpha}(\lambda)b}\left[1-\exp\left(-2\,\overline{\alpha}(\lambda)b\right)\right]d\lambda \qquad (13)$$
$$= 1-\int_{line}P_\lambda\,\overline{\alpha}(\lambda)b\,d\lambda+\int_{line}\frac{2}{3}P_\lambda\,\overline{\alpha}^2(\lambda)b^2\,d\lambda-\ldots.,$$

and the population escape factor for isotropic radiation becomes

$$\Theta_p = 1-\frac{\int_{line}\varepsilon_\lambda\left[1-\exp(-\overline{\alpha}\,b)\right]d\lambda}{\varepsilon_L} = \int_{line}P_\lambda\,\exp(-\overline{\alpha}\,b)\,d\lambda \qquad (14)$$
$$= 1-\int_{line}P_\lambda\,\overline{\alpha}(\lambda)b\,d\lambda+\int_{line}\frac{1}{2}P_\lambda\,\overline{\alpha}^2(\lambda)b^2\,d\lambda-\ldots..$$

2.3 Spectral Line Profiles

The following spectral line profiles have been included in the calculations: (p1) simple Doppler profiles, (p2) Lorentz profiles and (p3) Holtsmark profiles. They are given in Table 2 as a function of their full half-widths w. In addition, convolutions of Doppler and Lorentz profiles (Voigt profiles) and convolutions of Doppler and Holtsmark profiles have been provided in the program. The respective integration is carried out in the subroutine "voigt". Two superimposed Doppler profiles with different widths can be used to account for thermal or Franck-Condon and charge-exchange contributions to the emission.

Table 2: Options for spectral line profiles in the escape factor program, required input parameters and recommended spectral integration limits.

case	spectral line profile (nm^{-1})	parameters	integration limit
p1	$P_{\lambda,D}(\Delta\lambda) = \frac{1}{1.06446\, w_D} \exp\left[-\left(\frac{\Delta\lambda}{0.60056\, w_D}\right)^2\right]$	w_D (nm)	2.1 w_D
p2	$P_{\lambda,L}(\Delta\lambda) = \frac{2}{\pi w_L} \frac{1}{1+\left(\frac{2\Delta\lambda}{w_L}\right)^2}$	w_L (nm)	100 w_L
p3	$P_{\lambda,H}(\Delta\lambda) = \frac{2}{2.64261 w_H} \frac{1}{1+\left(\frac{2\Delta\lambda}{w_H}\right)^{2.5}}$	w_H (nm)	50 w_H
p4	Voigt profile	w_D, w_L	200 w_L
p5	convolution of Doppler and Holtsmark profiles	w_D, w_H	80 w_H
p6	sum of two Doppler profiles	$w_{D.1}$, $w_{D.2}$, $P_{D.2}(0) / P_{D.1}(0)$	3 $w_{D.2}$

As an example, Fig. 1 shows a Doppler and a Lorentz profile, as well as their resulting Voigt profile on a semi-logarithmic scale. The Doppler width corresponds to a temperature of 1 eV, a wavelength of 100 nm and the deuterium mass. The width of the Lorentzian is one fifth of w_D. All profiles are normalised to area one. The integration over wavelength in the course of escape factor calculations is carried out numerically, which means that arbitrary spectral profiles can be used, even as tabulated values. It is also possible to deal with overlapping lines.

According to Eq. 6, the line profiles can now be calculated for various optical thickness'. Figure 2 and 3 demonstrate the effect of self-absorption for the spatial emission cases (e1) and (e3), i.e. constant and parabolic form of the emission coefficient. In (e1) the source function $\varepsilon_\lambda / \overline{\alpha}$ is constant and therefore, the spectral line shape becomes flat in the centre, while self-reversal is found in case (e3) and also in case (e2) due to a decrease in source function height between the centre and the edge of the plasma. The depression of the line centre, e.g. for (e1) and $\overline{\alpha}(0)b = 1$, can be easily calculated from Table 1 to be $\frac{1}{2}(1-e^{-2}) = 0{,}4323$.

Asymptotically, $\varepsilon_\lambda(0)$ falls with $\frac{1}{\bar{\alpha}(0)b}$ in case (e1) and with $\frac{1}{\bar{\alpha}^2(0)b^2}$ in cases (e2) and (e3).

After integration of the spectral line profiles, the line escape factor is readily worked out. Examples for Doppler and Lorentz profiles, and for the three cases (e1) - (e3) are shown in Fig. 4. When the Lorentz profile is chosen, the calculation must be extended far into the line wings, because of their slow fall-off with wavelength. Figure 4 was calculated over 100 full half-widths to one side. The emitted radiation is highest for a constant spatial emission coefficient. If the emission is lower at the plasma edge, as in the cases (e2) and (e3), less optically thick radiation is emitted from the surface of the plasma and the corresponding escape factor is smaller. Linear and parabolic profiles behave very similarly here.

The results for the line escape factor and, as will be shown further down, also for the population escape factor apparently depend very critically on the spectral line profiles used and therefore, the profile shape must be an accessible input parameter for a general version of the program. It should be noted that in the present version of the main routine, the half-widths are assumed to be proportional to the centre wavelengths of the lines, as is the case for Doppler broadening.

2.4 Models for the Plasma Geometry

Again, three options are available for the plasma geometry, namely, (g1) an isotropic sphere with radius b (this does not require any additional calculation, since the solid angle integral is just 4π), (g2) a plane-parallel disk of thickness $2b$ and a prescribed diameter $2a$ and (g3), a cylinder with radius b and a prescribed length $2a$. The two latter geometrical models are shown in Fig. 5. Without further modification, the line escape factors described above immediately apply to the radiation emitted radially from the cylinder or perpendicular to the disk surface. For any other direction, the length must only be increased by $1/\sin\varphi$, as defined in Fig. 5. This does not warrant an extra input parameter. The population escape factors for the isotropic case (sphere) and various line and spatial emission profiles are shown in Fig. 6. In this case, the absorption of light in the centre originating from outer plasma zones is highest in the constant emission case, and therefore this population escape factor is at the lower side of the range.

The integration over the solid angle in the plasma is done numerically in the program according to the scheme indicated in Fig. 5. The angle ϑ is used as variable and x calculated accordingly. The element $d\Omega$ follows from the projected area and the distance to the centre point, which also determines the true length in the radiation transport equation. Care has been taken to arrive at precisely 4π after the Ω integration. Therefore, a correction has been implemented to account for the rim of the disk and the end planes of the cylinder by using appropriate average values. With these corrections, even cases with $a/b = 1$ can be treated with sufficient accuracy. In the following examples, the disk radius b is only twice its thickness a (with the exception below) and the half-length of the cylinder a is five times its radius b. Of course, once the optical depth is substantial, the results do not depend any more of the value of a, since the absorbed radiation in the centre of the plasma comes from the immediate neighbourhood.

Figure 7 represents examples of the population escape factors for the three geometry cases, a parabolic emission profile and the convolution of a Doppler and a Holtsmark profile with a width ratio of 5/1. Apparently, for the same shortest distance to the boundary, the arriving radiance in the plasma centre is higher for the disk, than the cylinder, and lower for the sphere, í.e. the escape factor is lower or higher, respectively, as would be expected from simple geometrical reasons. The slope of Θ_p over $\overline{\alpha}(0)b$ first corresponds to the Gaussian and later, with increasing optical thickness, to the Lorentzian, due to the profile convolution used.

The calculation in Fig. 8 was carried out for a comparison with the results published by Irons [1]. Therefore, a simple Doppler profile and spatially constant emission was used. In addition, the diameter of the disk was increased to five times its thickness, in order to be compared with Irons' results for an infinite slab. It must be noted that the thickness of the slab in his x-axis corresponds to $2b$ in the present calculations, such that his results have to be used at $x/2$. Figure 8 shows Irons' results for the "lower limit" (constant emission) and the two geometries in comparison with the present calculations. As is evident from Fig. 8, the agreement is perfect.

2.5 Modification of ADAS adf04 Data Sets for Collisional-Radiative Model Calculations

The population escape factors, obtained in the described way, have always been used to modify transition probabilities in ADAS adf04 data sets for subsequent collisional-radiative population calculations including opacity effects. For this purpose, the escape factor program first reads in the parameters for the normalised escape factor calculations, i.e. spectral line profile and plasma geometry information. In the present version, all input data are stored in a file containing the parameters for many runs performed in the past, which can thus be repeated any time for later reference. One of these cases is selected interactively and the line and the population escape factors are calculated and displayed as a function of $\overline{\alpha}(0)b$. Next, the program opens the adf04 file defined in the input parameter set. From the energy levels in this file it calculates the transition wavelengths and from the A-values and statistical weights the integrated absorption coefficients for density one. In order to derive the relevant lower state population from the provided total density of the species, the program must know the population of excited states including metastable levels. For this purpose, a Boltzmann distribution according to the input electron temperature T_e is adopted and separate underpopulation factors for metastables and other levels are applied. The actual ground state density is calculated by re-normalising the total population. As a further parameter, the spectral profile height in the line centre is required, which is derived from the normalised value of $P_\lambda(0)$ and a width corresponding to the Doppler width for the input gas temperature and species mass. Together with the length parameter b from the input file, the relevant product $\overline{\alpha}(0)b$ for each transition is now worked out and the population escape factor obtained by a quadratic, logarithmic interpolation of the normalised results. The A-values in the adf04 file are modified accordingly and replaced in the respective line, and the data are written to the defined output data set with an appended comment on the details of the relevant parameters of the run.

During the above calculation, the escape factor program displays the actual or anticipated

changes in the adf04 file by means of text and graphical output. An example of the latter is shown in Fig. 9 for the conditions of the neutral hydrogen measurements described in the next paragraph. Input parameters are deuterium, T_e = 1 eV, T_g = 2 eV, a neutral density of $3 \cdot 10^{19}$ m^{-3}, a length b of 5 cm and a Boltzmann distribution of the excited states (underpopulation factor = 1). The spectral line profile is the convolution of a Doppler and a Holtsmark profile widths $w_D/w_H \approx 5$. The spatial emission profile is parabolic and the cylindrical geometry has been chosen. Figure 9 shows the normalised line and population escape factors with the actual x-value for each hydrogen line of the run marked by a vertical line (third graph of "adasescape"). From Fig. 9 it can be concluded that the line escape factor for L_β and the chosen conditions is close to 0.5. Figure 9 also shows that the Paschen and Bracket lines may well become optically thick at higher electron temperatures, if the underpopulation is not substantial. H_α is optically thin in the case presented, even for a Boltzmann distribution, which is certainly an over-estimate for low-density plasmas. The line and the population escape factors are always very close together for a parabolic emission profile and cylindrical geometry.

3. Neutral Densities in the ASDEX Upgrade Divertor and Net Recombination Factors

In ASDEX Upgrade discharges approaching the density limit, the divertor plasmas near the target plates become cold and dense, the flows stagnate and the electrons and ions start to recombine effectively in the plasma volume. This leads to substantial neutral densities in the divertor region and the hydrogen Lyman lines become optically thick with all the consequences for ionisation balance and radiation. The onset of recombination into excited levels manifests itself clearly in the changing ratio of the hydrogen line intensities. Under such circumstances, the hydrogen Balmer radiation is mainly a function of the electron and ion densities, which can thus be derived from line or continuum intensities. The only simple method for measuring the neutral hydrogen ground state density consists of analysing the absorption or self-absorption of the Lyman resonance lines.

The so-called boundary-layer spectrometer on ASDEX Upgrade observes the divertor region from the mid-plane, both in the visible and the vuv wavelength regions and, during the divertor I campaign, almost perpendicular to the target plates. The hydrogen lines H_α and L_β (branching ratio transitions) emitted from the divertor region were recorded simultaneously during density ramp-up in many plasma discharges, either with fixed lines-of-sight or scanning across both divertor plates. With increasing density, the ratio of the two lines changed both in the inner and in the outer divertor typically by about a factor of 2 between low densities and $\bar{n}_e \approx 10^{20}$ m^{-3}, which can only be due to optical thickness of L_β. On the basis of the present opacity calculations, an approximate value for the neutral density can be derived from this result.

The spectral line profile of L_β is determined by Doppler broadening with several possible contributions, but also by Zeeman splitting and by the linear Stark effect. The latter two mechanisms have been investigated by Günter [6] for the relevant electron densities and the magnetic field of 2 T. As an example, the result for $n_e = 3 \cdot 10^{20}$ m^{-3} is shown in Fig. 10, which demonstrates that that the Zeeman and fine structure splitting alone produce a full half-width of about 3 pm. The ion temperature in this case is of the order 1 eV, such that a Doppler width

of roughly 5 pm is expected for deuterium, possibly somewhat higher due to the Franck-Condon energy after dissociation of the hydrogen molecules. Any cold component would at least have the Zeeman splitting and the Stark effect. The far wings of the L_β calculation roughly correspond to a Holtsmark profile of 1 pm full width, which theoretically scales as $n_e^{2/3}$. Therefore, for an approximate analysis of the measured data, the convolution of a Doppler profile with 7 pm width and a Holtsmark profile with w_L = 1 pm have been used. The Holtsmark wings are still of relatively low importance at the considered electron densities. All-together, the spectral line profile should not represent a major source of uncertainty in the neutral density analysis.
For determining the neutral density, the effective length of the emitting and absorbing plasma layers must be known. For an estimate of this length and for a judgement of the line-of-sight integrals, code simulations for a similar plasma discharge are shown in Fig. 11 [7]. This figure represents two-dimensional results for the intensity of H_α emission in the outer leg of divertor I, as well as the distribution of hydrogen neutrals in the divertor region. A selection of sight-lines of the boundary-layer spectrometer is also plotted. The modelled discharge is an L-mode case with 4 MW additional heating. The electron density in the mid-plane at the presented time slice is $\approx 3.9 \cdot 10^{19}$ m^{-3} and the divertor density is $\approx 4 \cdot 10^{20}$ m^{-3}. The H_α emission is particularly high close to the surface of the target plate and extends for some 5 cm along the sightline of the boundary-layer spectrometer. The neutral densities are fairly uniform and the highest values also extend over a few cm length. It should be noted that, according to the calculations, there is another patch of high neutral density near the X-point, due to Marfe formation. In the inner divertor, the effective lengths are about twice as long, due to the divertor and sightline geometries, as shown by these calculations and an analysis of the absolute line intensities [8]. For the present example 5 cm are being used as the effective (half-) lengths of the emitting and absorbing layers. The higher emission near the target plate, as shown by the code simulation in Fig. 11, may result in a slight over-estimate of the neutrals. For evaluating the line escape factor, a parabolic emission profile has been used and the results in Fig. 9 have been obtained with the described combination of input parameters. The escape factor for L_β is 0.5, which agrees with the typical optical thickness. Therefore, the result for the average neutral hydrogen density is $n_0 \approx 3 \cdot 10^{19}$ m^{-3}, a value, which is in very good agreement with the divertor code calculations predicting 2 - 5 $\cdot 10^{19}$ m^{-3}. The most important source of uncertainty in this analysis is the emission geometry, which could be adapted more precisely for selected plasma discharges in future measurements.

The consequences of opacity on hydrogen ionisation balance and line emission have already been investigated in [4]. It should be noted that the calculations in [4] were carried out only including levels with principal quantum numbers up to n = 5. Subsequently, the effect of very many higher lying states has been taken into account by using the so-called projection matrix in the ADAS208 collisional-radiative population calculations. Including this matrix changes the results in [4] somewhat in their absolute value. With increasing n, higher states are better coupled to the free ions, taking the results for n = 3, n = 4 and n = 5 further apart. Ionisation and recombination coefficients are also somewhat higher. However, the basic conclusions described in [4] remain applicable. Another report on the status of hydrogen radiation and S/XB data is in preparation, which will make use of the complete atomic physics data sets.

For analyses of high density divertor plasmas, an important quantity is the net plasma recombination, i.e. recombination minus ionisation, reducing the ion flux to the target plates. The net recombination coefficient can be evaluated on the basis of the ADAS hydrogen

calculations for optically thin and optically thick conditions. It depends on electron density, ionisation degree and optical thickness of the resonance lines. We define α_{eff}:

$$\alpha_{eff} = \alpha(T_e,n_e) - \frac{n_0}{n_i} S(T_e,n_e) = \alpha(T_e,n_e) - \frac{1}{\kappa} S(T_e,n_e)\,, \qquad (15)$$

with the recombination rate coefficient α, the ionisation rate coefficient S and the ionisation degree κ. Examples for α_{eff} are presented in Fig. 12 vs. temperature for two values of n_e and ionisation degrees of 1, 10 and ∞. Figure 12 demonstrates that net recombination can only take place at electron temperatures below about 1.5 eV, unless the ionisation degree is extremely high. From measurements and from modelling one would expect κ to be about 10 - 20, and the electron temperature must therefore be in the 1 eV region, which is also found experimentally. Opacity of the resonance lines just shifts all results to lower temperatues, because it increases the ionisation degree for a given T_e. These results of the present study represent a valuable basis for future code calculations including optical thickness.

4. Summary

Escape factors for spectral line emission along a given line-of-sight, Θ_L, and for collisional-radiative population calculations of excited levels in atoms and ions, Θ_p, have been calculated on the basis of some simplifying approximations by means of the PC computer program "adasescape". A wide choice of spectral line profiles, spatial emission profiles and plasma geometry cases is available in this code. Doppler, Lorentz or Holtsmark profiles can be used, as well as convolutions and superposition of different types and widths, in order to account for various line broadening mechanisms and particle groups with different temperatures. The spatial emission profiles of radiation are approximated by a polynomial fit and examples are given for constant emission, as well as a linear or a parabolic decrease from the plasma centre to the edge. The population escape factors can be calculated in the centre of a plasma sphere, in the mid-plane of a disk, or on the axis of a cylinder. Examples of normalised escape factors for Θ_L and Θ_p and for a variety of cases have been described in this report and the consequences of the different models have been discussed. The results have been applied to a measurement of the neutral hydrogen density in ASDEX Upgrade divertor I from the self-absorption of L_β. For this purpose, a calculation of the L_β line profile was used, which includes Zeeman splitting for the relevant magnetic field and Stark broadening for the plasma electron density. The geometrical form of the emission zone and of the neutral hydrogen cloud were taken from model calculations of the ASDEX Upgrade divertor plasma. The result for the neutral hydrogen density is in very good agreement with expectations on the basis on the model calculations. The self-absorption of Lyman lines is a reliable experimental tool for measurement of neutral hydrogen densities in divertor plasmas, which can be further improved by accompanying code simulations. In the future, the essential content of the escape factor program will be included in the ADAS atomic data base. Using ADAS, hydrogen radiation, S/XB ratios, as well as ionisation and recombination coefficients can be calculated including plasma opacity. In this report, an example has been presented for hydrogen net recombination factors as a function of electron temperature and density, of ionisation degree and of optical thickness of the resonance lines.

References:

[1] F.E. Irons, The Escape Factor in Plasma Spectroscopy - I. The Escape Factor Defined and Evaluated, JQSRT **22**, 1 (1979)

[2] SFB 259, Bericht über Hochtemperaturprobleme rückkehrfähiger Raumtransportsysteme, Arbeits-u. Ergebnisbericht, Universität Stuttgart, 1992

[3] H. Jentschke, Spektroskopische Untersuchung eines luftähnlichen Plasmafreistrahls, Thesis, Institut für Plasmaforschung, Universität Stuttgart, 1995

[4] K. Behringer, The Influence of Opacity on Hydrogen Line Emission and Ionisation Balance in High Density Divertor Plasmas, IPP 10/5, 1997

[5] H.P. Summers, L. Wood, Ionisation, Recombination and Radiation of Impurities in Plasmas, JET Report, JET-R(88)06 (1988), ADAS Data Pool (Atomic Data and Analysis Structure), Editor H.P. Summers (1993)

[6] S. Günter, private communication, IPP 1998

[7] R. Schneider and D. Coster, private communication, IPP 1998

[8] U. Wenzel et al., Plasma Parameters and Volume Recombination in the ASDEX Upgrade Divertor I, to be published 1998

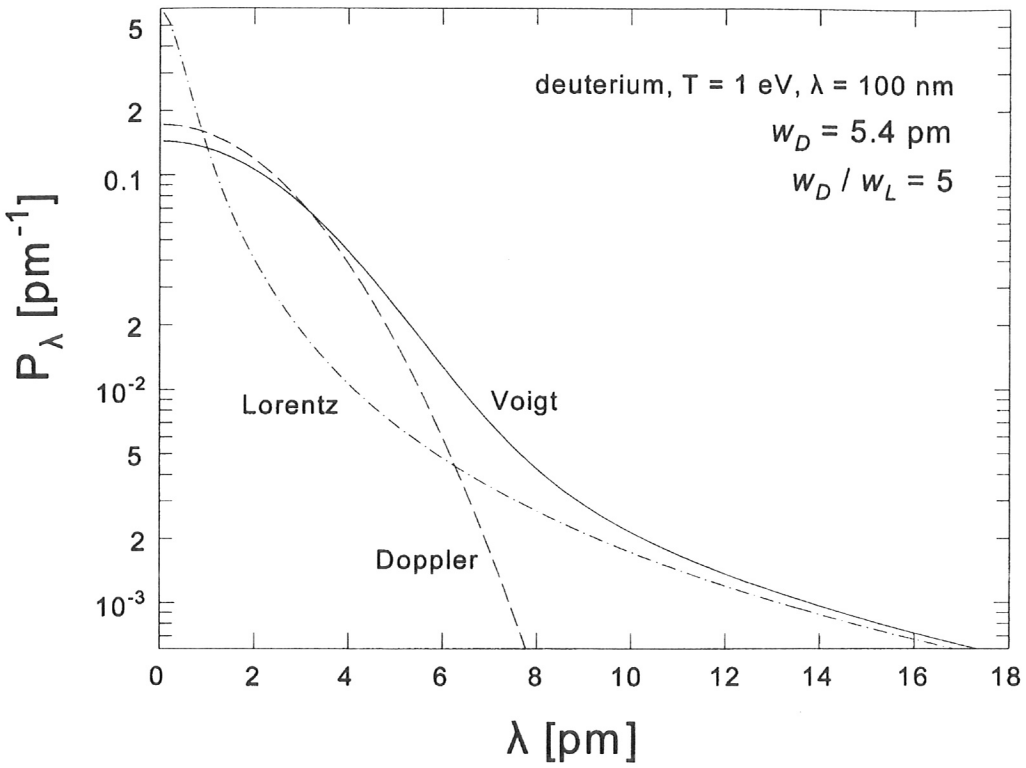

Fig. 1: Examples of Doppler and Lorentz profiles, as used in the escape factor code, and their convolution to a Voigt profile.

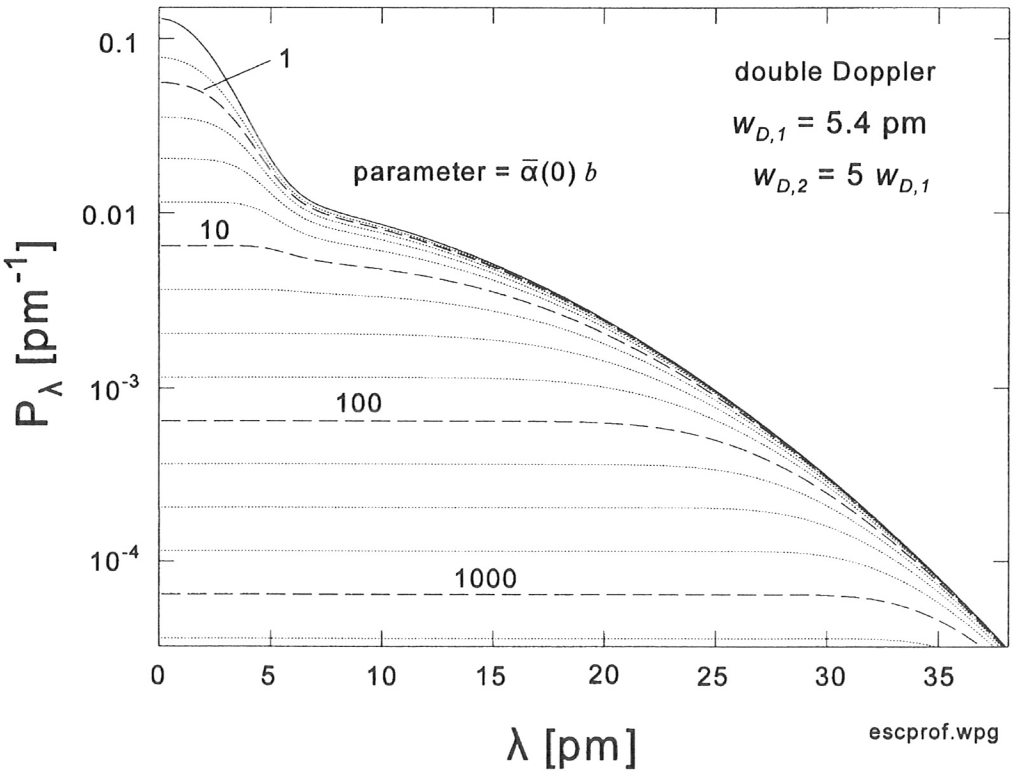

Fig. 2: Example for the calculation of spectral line profiles with various values of optical thickness. Shown is the superposition of two Doppler profiles for an emission coefficient, which is independent of plasma radius (case e1).

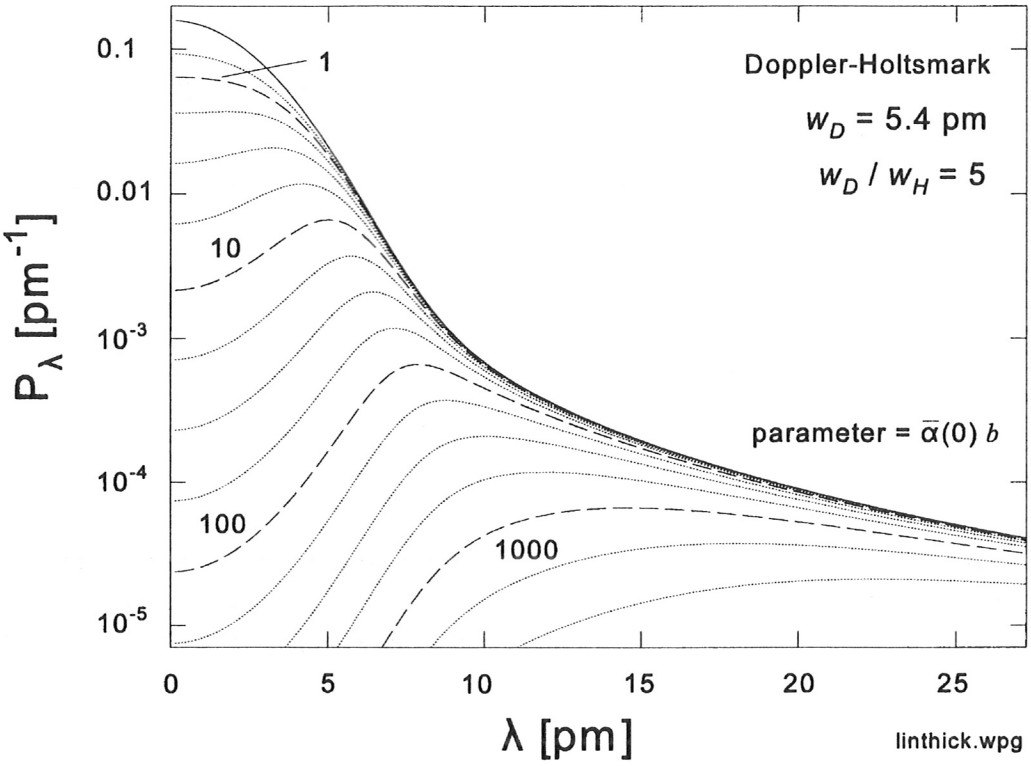

Fig. 3: Example for the calculation of spectral line profiles with various values of optical thickness. Shown is the convolution of a Doppler and a Holtsmark profile. The emission coefficient as a function of the plasma radius has a parabolic shape (case e3).

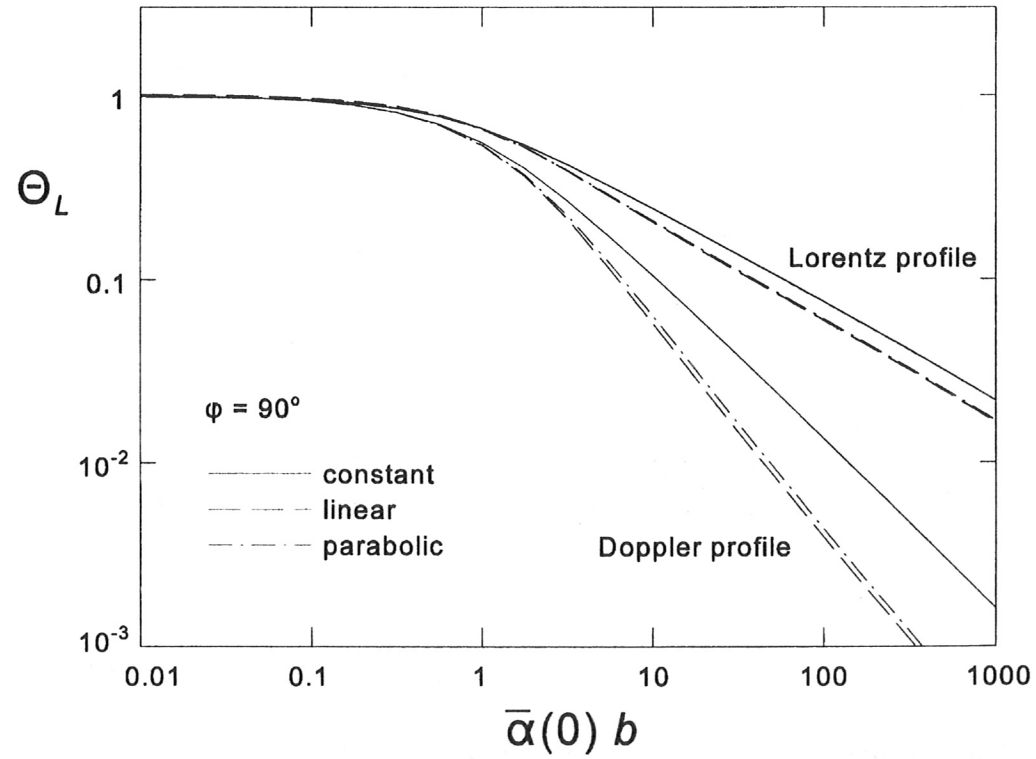

Fig. 4: Escape factors for perpendicular line emission. The influence of Doppler or Lorentz profiles is demonstrated, as well as the consequences of spatial emission profiles (cases e1, e2 and e3).

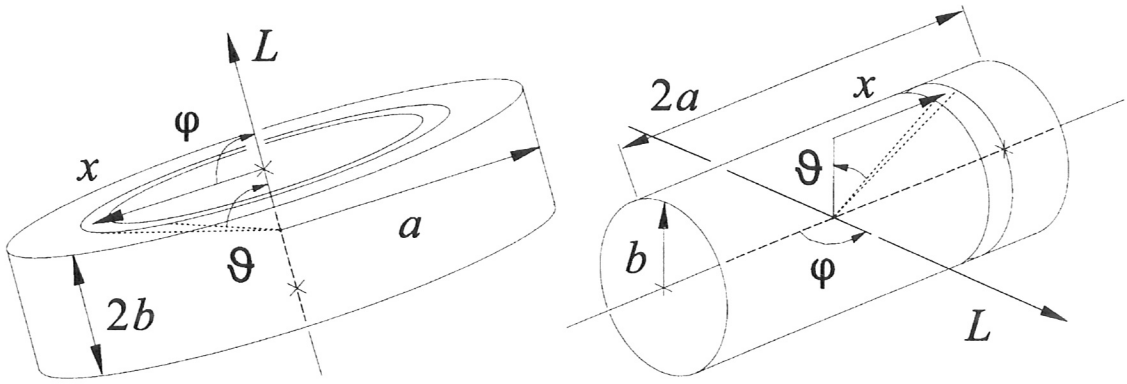

Fig. 5: Geometry for cases (g2), disk or slab, and (g3), cylinder. Explanation of the integration over solid angle for calculating the population escape factor. The spatial profiles of the emission coefficient, as well as the line escape factor apply to the direction of b.

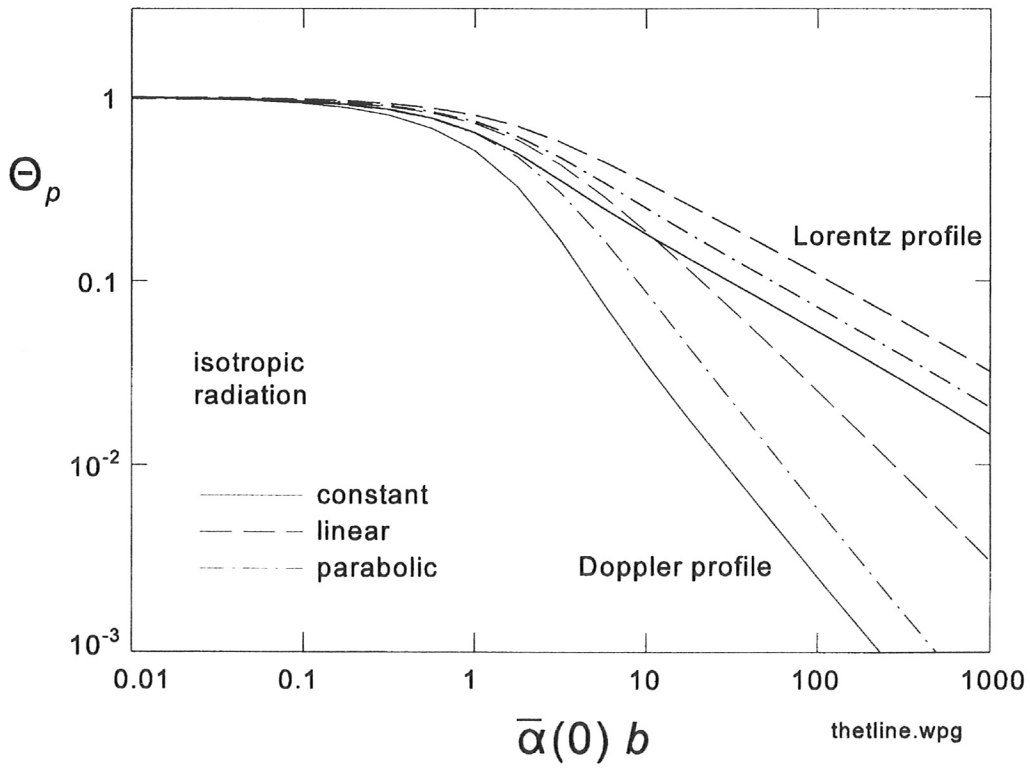

Fig. 6: Escape factors for population calculations. Isotropic case (sphere, g1). The influence of Doppler or Lorentz profiles is demonstrated, as well as the consequences of spatial emission profiles (cases e1, e2 and e3).

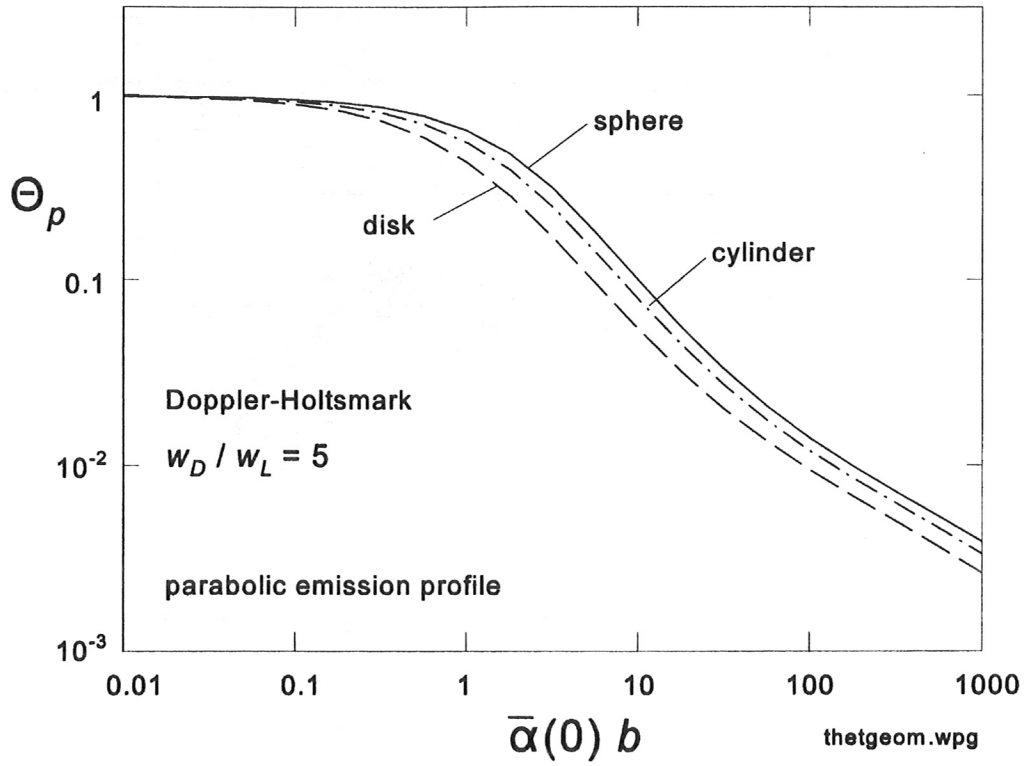

Fig. 7: Population escape factors for the three geometrical plasma models (g1) sphere, (g2) disk, and (g3) cylinder. The convolution of a Doppler and a Holtsmark profile is being used and the emission case is parabolic (e3).

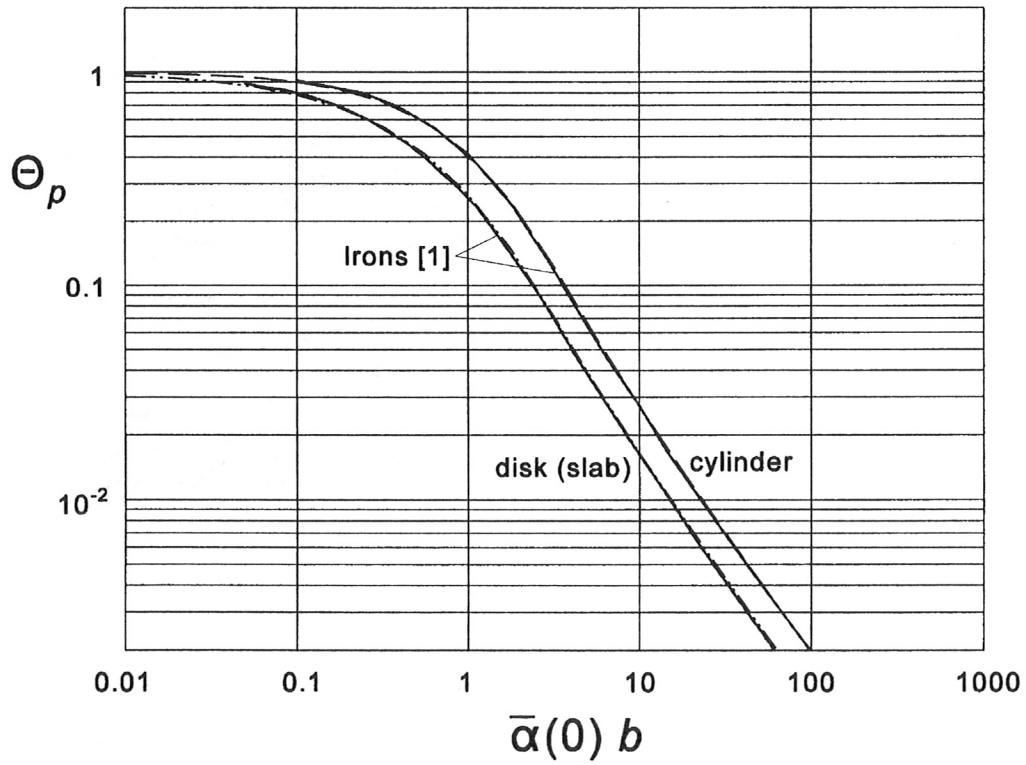

Fig. 8: Population escape factors for spatially constant emission and cylinder or disk geometries (slab with thickness 2b). A comparison with the results published by Irons [1] shows perfect agreement.

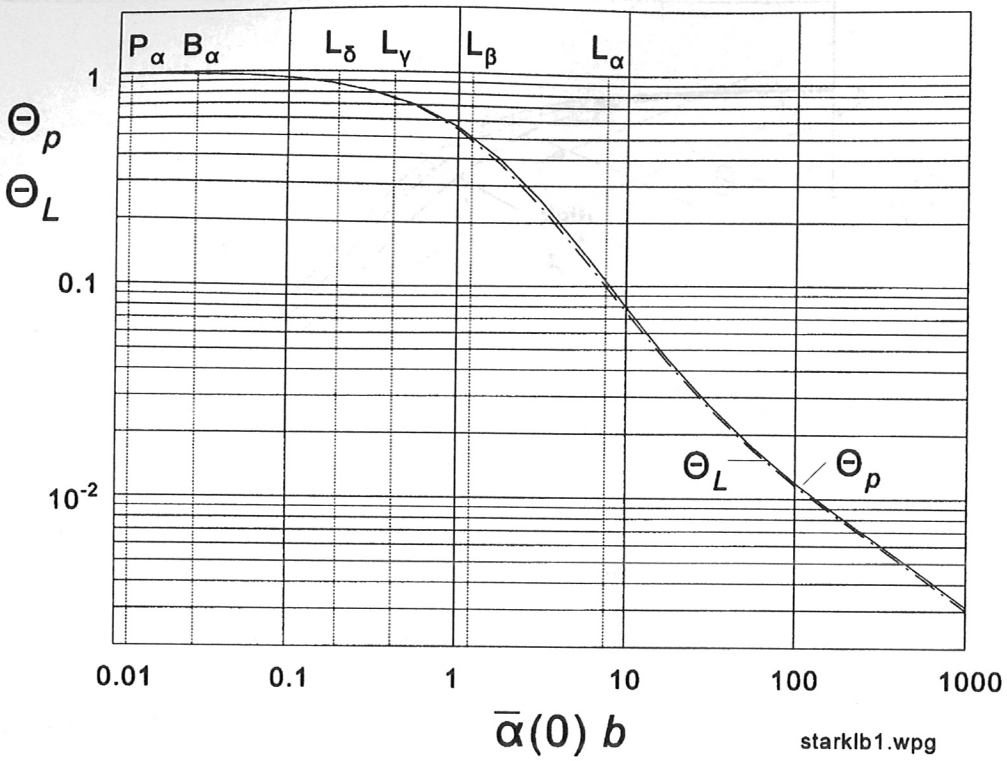

Fig. 9: Population and line escape factors for neutral density measurements in the ASDEX Upgrade divertor I. See text for the parameters of the calculations. The values for the hydrogen Lyman lines, as well as P_α and B_α are marked (Boltzmann distribution).

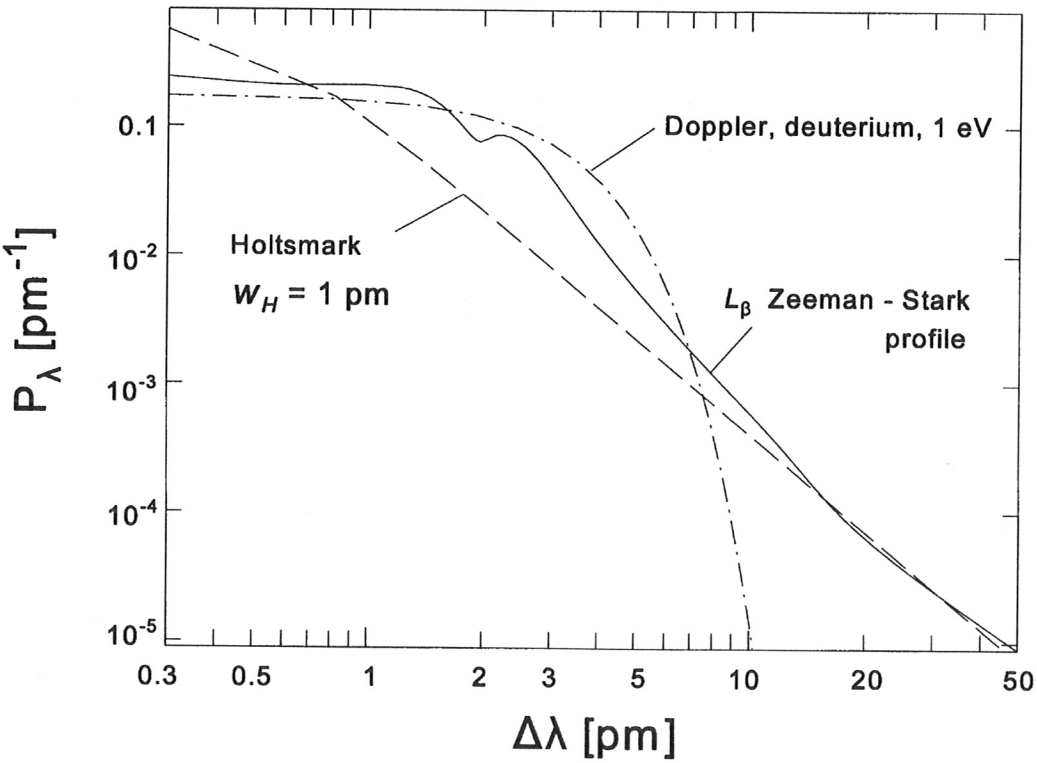

Fig.10: Spectral line profile for L_β including Zeeman splitting for a magnetic field of 2 T and Stark effect for $n_e = 3 \cdot 10^{20}$ m^{-3} after Günter [7]. Also shown is a Doppler profile for deuterium, 1 eV and 100 nm, as well as a Lorentz profile with 1 pm full half-width.

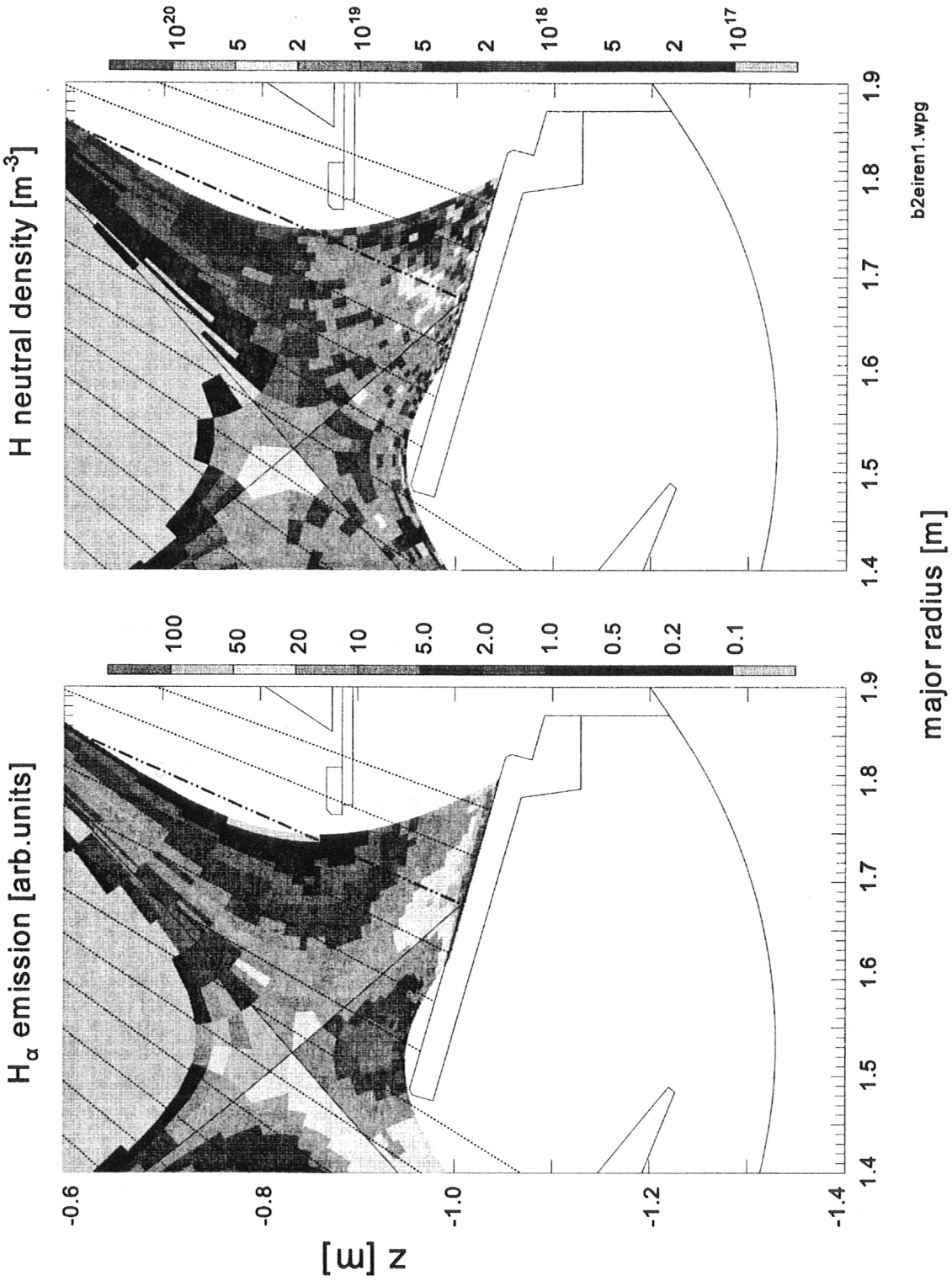

Fig.11: Results of code calculations for the density of neutral hydrogen atoms and for the emission of H_α in ASDEX Upgrade divertor I. L-mode discharge with 4 MW additional heating. The predicted electron densitiy in the divertor is about $4 \cdot 10^{20}$ m^{-3}. These calculations are used as a guidelines for anaylysing the optical thickness measurements. A sightline of the boundary-layer spectromer is marked which would have maximum signal. The predicted maximum neutral densities in the modelled case are 2 - $5 \cdot 10^{19}$ m^{-3}.

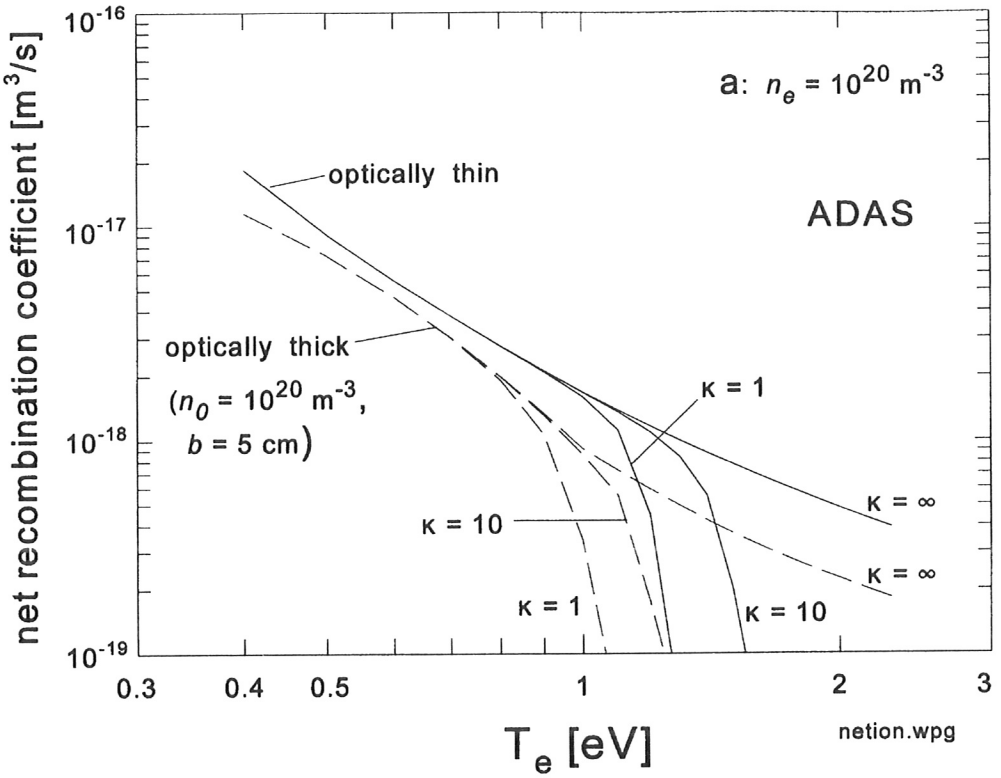

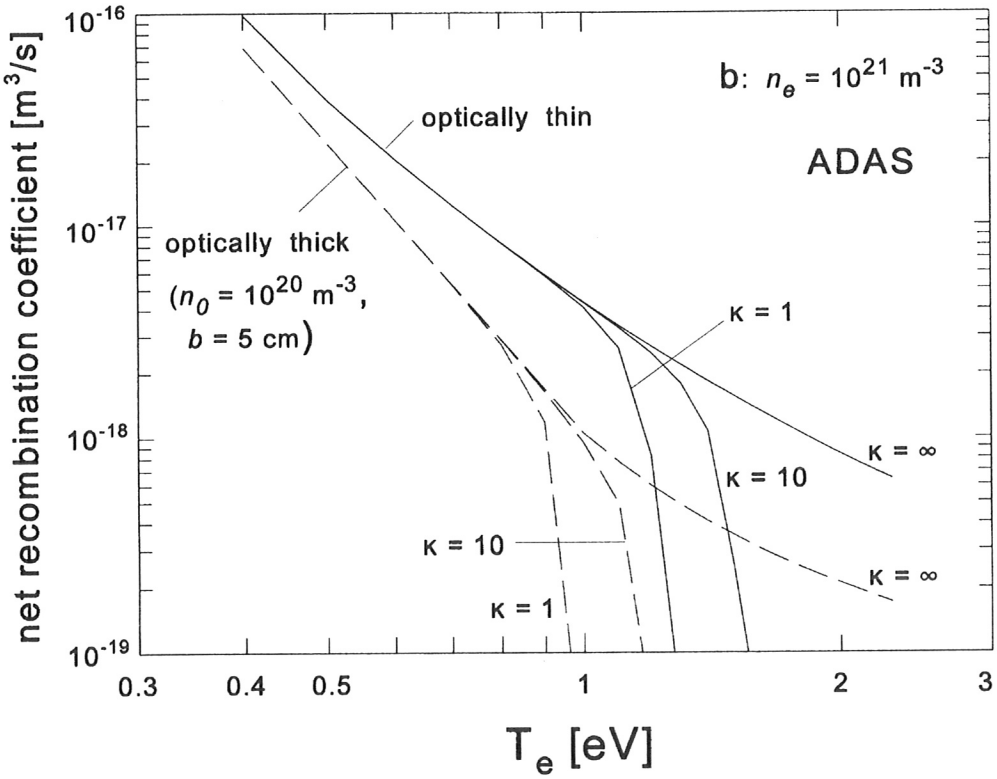

Fig. 12a and 12b: Hydrogen net recombination factors as a function of electron temperature and density, of ionisation degree $\kappa = n_i / n_0$ and of opacity of the resonance lines. Optical thickness, which is assumed to be an independant parameter, shifts the results to lower temperatures.